

Vol. 9. No.3. 2020

©Copyright by CRDEEP Journals. All Rights Reserved.

Contents available at:

[www.crdeepjournal.org](http://www.crdeepjournal.org)

International Journal of Environmental Sciences (ISSN: 2277-1948) (CIF: 3.654)

Full Length Research Article

## Isolation and Crystal Structure determination of Tetragonal Crystal System of Mixed Valence $\text{Bi}_{0.5}\text{Mn}_{0.64}\text{Mo}_{1.5}\text{O}_{0.41}$ oxide by Powder XRD

Bimal K.Kanth and Parashuram Mishra\*

Bioinorganic and Materials Chemistry Research Lab., Tribhuvan University, M.M.A.M.Campus Biratnagar, Nepal.

## ARTICLE INFORMATION

## ABSTRACT

**Corresponding Author:**

Prashuram Mishra

**Article history:**

Received: 26-07-2020

Revised: 08-08-2020

Accepted: 13-08-2020

Published: 18-08-2020

**Key words:**

X-ray, spectroscopy,  
complex oxide,  
quenched  
Compaction Factor and  
Split Tensile.

In the course of the exploration of the  $\text{Bi}_2\text{O}_3$ - $\text{MnO}_2$ - $\text{MoO}_4$  ternary phase diagram, a new compound with the formula  $\text{Bi}_{0.5}\text{Mn}_{0.64}\text{Mo}_{1.5}\text{O}_{0.41}$  was discovered. Its structure was determined from a powder X-ray diffraction data. It crystallizes in the tetragonal space group  $P4/mmm$  with the lattice parameters:  $a=9.6076 \text{ \AA}$   $c=8.2616 \text{ \AA}$ . The structure refinement converged to  $RF55.043$  and  $R \text{ Bragg}52.047$ . The structure is built from cationic slabs parallel to  $(100)$  faces of the tetragonal cell. Each cell corresponds to one slab containing a mixed  $\text{Bi}_{0.86}\text{Mn}_{1.14}$  cationic layer ( $\text{Bi}(1)$ ) sandwiched between two equivalent bismuth layers ( $\text{Bi}(2)$ ). The cohesion of the cations in the slabs results from the presence of the oxygen atoms distributed over three sites. Six  $\text{O}(1)$  and two  $\text{O}(2)$  atoms form a slightly distorted cubical polyhedron around the mixed cationic site ( $\text{Bi}(1)$ ).  $\text{Bi}(2)$  atoms are surrounded by seven oxygen atoms in a very distorted polyhedron. The important delocalization of  $\text{Bi}(2)$  lone pairs toward the interslab spaces leads to significant bonds with the adjacent slabs and to the cohesion of the structure.  $\text{Bi}_{0.5}\text{Mn}_{0.64}\text{Mo}_{1.5}\text{O}_{0.41}$  is the low symmetry variety of a particular sample of a wide solid solution domain that, formulated  $\text{Bi}_{0.5}\text{Mn}_{0.64}\text{Mo}_{1.5}\text{O}_{0.41}$  has been investigated. The formation of this phase from the irreversible transformation of quenched- $\text{b}_1$  on heating and the subsequent transitions  $\text{Mo}_1\text{Mo}_2$  have been evidenced by thermo diffractometry, conductivity measurements versus temperature, dilatometry, and thermal analyses. The electrical properties of this compound were investigated on sintered pellets by means of complex impedance spectroscopy.

**Introduction**

In materials science, the crystal structure determination is the first step to understand and interpret physical properties of an unknown material. Moreover, it also guides people on how to modify the material and hence improve the performance. Nowadays, the most successful technique for structure determination is through single crystal X-ray diffraction, from which a sufficient number of independent reflections against the structural parameters can be extracted in 3D reciprocal space. Several mature analysis methods, such as the direct method,<sup>1</sup> Patterson method,<sup>2</sup> charge-flipping algorithm<sup>3</sup> and maximum entropy method can be applied to accurately solve the structure<sup>[1]</sup>. This technique requires synthesizing a high quality single crystal at a micrometer level, which might be difficult in some fields, for example in ceramic chemistry. Experimentally, the chance to get polycrystalline materials is generally larger than to get single crystals. In this case, powder X-ray diffraction (PXRD) becomes a popular technique but with this technique, the possibility to determine an unknown structure dramatically decreases, because 3D reflections are compressed into 1D with

an inevitable overlapping problem, especially when the unit cell is big.

The situation will become worse when the PXRD is collected on a multi-phase sample, which is not uncommon in the preliminary stage of searching new materials, especially in the cases of hydrothermal (or solvothermal) syntheses of zeolitic or MOF materials<sup>[2]</sup>. The difficulty could further increase when the target phase is not the highly dominant one in the composition. To determine the structure of an unknown phase in a multi-phase polycrystalline sample would be very helpful for the researchers, saving time to optimize the syntheses conditions. Against such a case, we successfully determined a metastable structure with the formula,  $\text{Bi}_{0.5}\text{Mn}_{0.64}\text{Mo}_{1.5}\text{O}_{0.41}$  which is in fact an intermediate phase during the decomposition of mullite-  $\text{Bi}_{0.5}\text{Mn}_{0.64}\text{Mo}_{1.5}\text{O}_{0.41}$  (solid solution of  $\text{Bi}_2\text{O}_3$ - $\text{MnO}$  and  $\text{MoO}_2$ <sup>[3]</sup>) Practically, there is a growing interest in  $\text{Bi}^{3+}$ -containing transitional metal oxides, as potential multiferroic materials since the employment of lone pair electrons and transition metals is the simplest and most natural way to combine magnetic and ferroelectric order. We

started with the exploration in the Bi–Mn–Mo–O phase diagram, and found the unknown phase 1 in the Mn rich area during the decomposing process of mullite  $\text{Bi}_{0.5}\text{Mn}_{0.64}\text{Mo}_{1.5}\text{O}_{0.41}$ . All the attempts to obtain a pure phase of 1 failed [4].

In view of this, it seems interesting to search for new phases belonging to the columnar  $\text{Bi}_{0.5}\text{Mn}_{0.64}\text{Mo}_{1.5}\text{O}_{0.41}$  structural type with the aim of improving the electrical response of these materials. So, the authors have undertaken the study of the possible solid solutions  $\text{Bi}_{0.5}\text{Mn}_{0.64}\text{Mo}_{1.5}\text{O}_{0.41}$ , taking into account the fact that Mn can adopt a tetrahedral coordination like that of Mo-O in this structures[5].

This article reports on the new phases obtained, as well as the structural characterization and electrical properties. While this paper was being written, the authors became acquainted with the structural and electrical study carried out by Grins *et al.* on Bi-Mn-Mo-O ternary oxide [6]. This new phase also exhibits a columnar [Bi-O-MnMo-O] structure, different from those previously reported,[7] which can be considered as the simplest case in the whole family, with columns only surrounded by isolated Mo-O tetrahedra. On the other hand, Bi-Mn- Mo-O has a maximum electrical conductivity is shown.

### Materials and methods

All the chemicals used were analytical grade. Typical synthesis process was conducted as follows. The initial polycrystalline mixture of starting materials  $[\text{Bi}_2(\text{CO}_3)_3, \text{MoCO}_3 \text{ and } \text{MnCO}_3]$  was ground with an agate mortar, pressed into a pellet and slowly heated up to 800 °C at a rate of 80 °C h<sup>-1</sup>. The resulting pellet was reground, repressed and heated at a higher temperature with intermediate regrinding steps. After every annealing process, the resultant sample was checked by PXRD. The PXRD data for the structure determination were collected on a PANalytical X'Pert Pro Alpha-1 equipped with a PIXcel detector (Cu-Kα1 radiation). Energy-dispersive X-ray spectroscopy (EDS) was performed using a JEOL 2100F transmission electron microscope[8]. The relative density of the sample before the mechanical grinding was 79 %. Platinum electrodes were connected to the two faces of the pellet via a platinum paste to keep good electric contacts. Impedance spectroscopy measurements were carried out using a Hewlett-Packard 4192a Impedance Analyzer. The impedance spectra were recorded in the 5 Hz-13 MHz frequency range. Electrical conductivity measurements of representative  $\text{Bi}_{0.5}\text{Mn}_{0.64}\text{Mo}_{1.5}\text{O}_{0.41}$  were carried out by complex impedance spectroscopy with a 1174 Solectron frequency response analyzer coupled to a 1286 Solartron electrochemical interface. Pellets of about 14 mm diameter and 1 mm thickness were prepared by cold pressing of a mechanically activated powder mixture with the composition:  $\text{Bi}_{0.5}\text{Mn}_{0.64}\text{Mo}_{1.5}\text{O}_{0.41}$  was form the phase, the pellets were heated at 7003C during 12 h and slowly cooled to room temperature. This synthesis method was employed to improve the ceramic quality, as it has been shown for other materials [9-].The formed phases and crystallinity were studied by X-ray powder diffraction. Platinum electrodes were deposited on the two faces by sputtering, and measurements were carried out in the temperature range 200-6503C, at steady temperatures, with pellets under air flow. The frequency range was fixed.The Rietveld refinement carried out JANA software package and density was measured by Archimedes principle.

### Results and discussion

Several attempts to grow single crystals of the title compound were unsuccessful, but the powder quality had to be improved to be suitable for powder XRD analysis. The powder resulting from the reaction of  $\text{Bi}_{0.5}\text{Mn}_{0.64}\text{Mo}_{1.5}\text{O}_{0.41}$  in air presents an average crystal size of 60 nm, which is too small for a satisfactory structure solution. As a mineralize, Mn ion was found to be helpful to increase the crystal size. Small amounts of Mo improved the crystal growth slightly. Finally, an almost single phase powder of  $\text{Bi}_{0.5}\text{Mn}_{0.64}\text{Mo}_{1.5}\text{O}_{0.41}$  was obtained with an average coherence length of Bi 120 nmThis sample was found to be suitable to solve the structure from conventional powder diffraction data. Indexing the 25 first reflections[10] (see Figure 1) gave an tetragonal unit cell. A whole pattern fitting using the Le Bail method,[11] after crystallographic transformations, suggested the space group *P4/mmm* as the one with the highest possible symmetry. The structure was solved in this space group by using the Diamond program package,[8] as described in the materials and methods . The starting model was based on five bismuth ions and two rigid MoO<sub>2</sub> ions octahedral. After convergence, the structure was refined with JANA (see Figure 2). The refinement parameters are summarized in Table 2 for 34 atomic coordinates and 3 isotropic temperature coefficients. Structural data are given in Table 3 and selected interatomic distances are given in Table 4 together with the calculated valence bond sum.[12,13] The values for Bi scatter between 1.6 and 2.7. The unusual high valence bond sum (VBS) of Mn+2 ion is probably related to the lowest coordination number 6 and short Bi–O distances. In difference to the other Bi ions in the structure, Bi3 is located in a tunnel-shaped arrangement of oxygen atoms parallel to the *b* axis. The high VBS value marks probably the limit of the stability of this structure. The VBS values for iodine are in the expected range (Table 4). Figure 2a shows the structural arrangement perpendicular to the *b* axis and Figure 2b the oxygen channel around Mo ion . The structure can be described by cations forming a two-dimensional network around an almost pentagonal hole, which is covered by the layers above and below. Oxygen atoms O5–O8 are located within the layer and oxygen atoms O1–O4 connect the different layers. All oxygen atoms are part of the two MoO<sub>2</sub> octahedra. The average Bi–O distance is 2.69(1) Å, the shortest distance Bi3–O8 was calculated to be 2.54(1) Å. Similar short distances were found in  $\text{Bi}_{0.5}\text{Mn}_{0.64}\text{Mo}_{1.5}\text{O}_{0.41}$  [14] Coordination numbers (and average distances) are 7 for Bi2 (2.64 Å), 10 for Bi1 (2.93 Å), Mn3 (2.89 Å), and Mo4 (2.87 Å) and 11 for Mo5 (3.02 Å). It should be noted that the coordination number of 7 around Ba2 is unexpected. Nevertheless a geometrically similar environment was observed around zirconium in monoclinic ZrO<sub>2</sub>. [17] The average Mo–O distances of the  $\text{Bi}_{0.5}\text{Mn}_{0.64}\text{Mo}_{1.5}\text{O}_{0.41}$  octahedral are 1.87 and 1.91 Å, as observed for other bismuth ions are shown in table 2

### Structure solution

#### Rietveld Refinement

The framework structure of  $\text{Bi}_{16}\text{Mn}_{12}\text{Mo}_3\text{O}_{16}$  was first examined by ab initio structure determination method using the powder XRD data. Refinene by JANA software The initial lattice parameters were determined to be parameters Bi16 Mn12 Mo3 O16, formula weight 4546.75 g/mol, crystal system Tetragonal, cell parameters a=9.6076 Å c=8.2616 Å, and volume=762.60 Å<sup>3</sup> space group is P 4/m m m (123) by an indexing procedure using

the program TREOR15 in EXPO2004.16 The most probable space group was suggested to be P 4/m m m (123) crystal system Next, the integrated intensities were extracted by the Le Bail method using the program Jana2006.14 A profile function and background function of the Le Bail method used in the present study were pseudo-Voigt function and 20<sup>th</sup> order Legendre function, respectively. An initial structure model was then obtained by the charge flipping (CF) method<sup>17</sup> using the extracted integrated intensities. Although the Mn site could not be clearly determined by the CF.

The iteration converged with an R factor of 25% and the final electron density shows a P 4/m m m (123) symmetry with a 5% error. The program of EDMA was then used to automatically assign atomic positions. Four unique heavy atomic positions were found and the heaviest one was assigned as Bi while the others were considered as Mn and Mo. Due to the existence of heavy atoms, all oxygen positions were ambiguous in the electron density map of this stage. To locate the oxygen atoms, a Monte-Carlo based simulated annealing process with the program Diamond package was applied. For each annealing process, various atomic coordinates were randomly assigned as the initial positions of the oxygen atoms [15-16]. The annealing process was restarted after finding a few oxygen positions, until all oxygen positions were found to be reasonable shown in figure 3.

**Table 1.** Crystallographic data

Formula sum	Bi <sub>0.5</sub> Mn <sub>0.64</sub> Mo <sub>1.5</sub> O <sub>0.41</sub>
Crystal system	tetragonal
Space-group	P 4/m m m (123)
Cell parameters	a=9.6076 Å c=8.2616 Å
Cell ratio	a/b=1.0000 b/c=1.1629
	c/a=0.8599
Cell volume	762.60 Å <sup>3</sup>
Z	2
Calc. density	9.89989 g/cm <sup>3</sup>
Meas. density	9.81233g/cm <sup>3</sup>
Pearson code	tP47
Formula type	A3B12C16D16
Wyckoff sequence	Tsroljihgea
Indexes	1 ≤ h ≤ -2, -2 ≤ k ≤ 0. -2 ≤ k ≤ 2

**Table 2.** Atomic parameters

Atom	Ox.	Wyc k.	Site	S.O.F.	x/a	y/b	z/c
Bi1	+3	4i	2mm.		0	1/2	0.17960
Bi1	+3	4j	m.2m		0.70690	0.70690	0
Mn1	+4	8s	.m.		0.81560	0	0.35050
Mo1	+2	1a	4/mmm		0	0	0
Bi1	+3	8r	.m		0.74270	0.74270	0.34260
Mo1	+2	2h	4mm		1/2	1/2	0.18280
Mn1	+4	4o	m2m.		0.72810	1/2	1/2
O1	-2	4l	m2m.		0.69940	0	0
O1	-2	8t	.m.		1/2	0.73770	0.23490
O1	-2	2e	mmm.		1/2	0	1/2
O1	-2	2g	4mm		0	0	0.19830

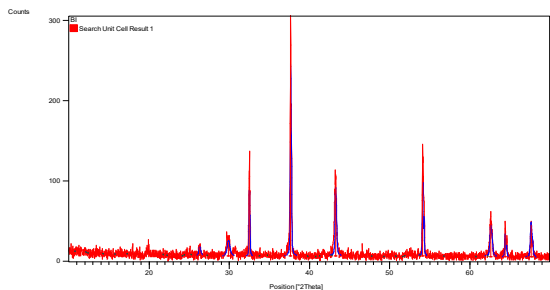


**Fig1.** Powder XRD spectra of Bi<sub>0.5</sub>Mn<sub>0.64</sub>Mo<sub>1.5</sub>O<sub>0.41</sub>

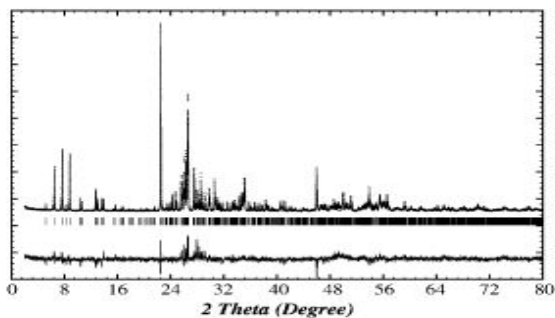


**Fig. 2.** Graphical representation of Bi<sub>0.5</sub>Mn<sub>0.64</sub>Mo<sub>1.5</sub>O<sub>0.41</sub> from Rietveld refinement with X-ray powder data. Vertical bars indicate positions of the Bragg reflections for of Bi16 Mn12 Mo3 O16, dots mark the observed intensities and the solid line gives the calculated intensity curve. The deviations between the observed and the calculated intensities from the refined model are shown by the difference plot in the lower part of the diagram.

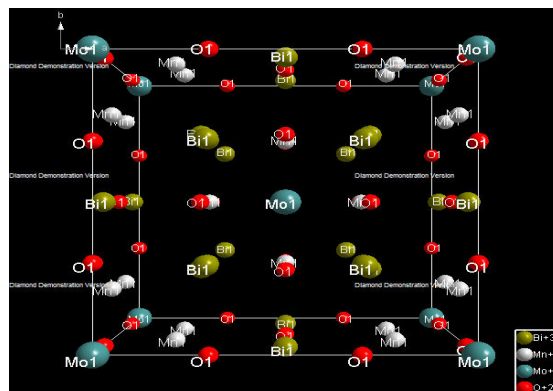


**Fig 3** Face centered tetragonal structure of Bi<sub>0.5</sub>Mn<sub>0.64</sub>Mo<sub>1.5</sub>O<sub>0.41</sub>

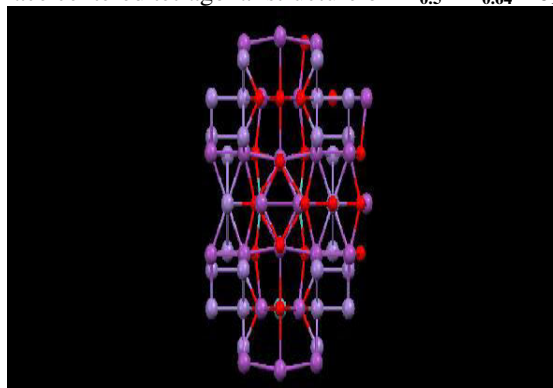


**Fig .3D** structure of Bi<sub>0.5</sub>Mn<sub>0.64</sub>Mo<sub>1.5</sub>O<sub>0.41</sub>

## Selected Bond angles

Atom1	Atom2	Atom code	Atom3	Atom code	Angle
Bi1	O1	8565041	O1	8555021	104.483
Mn1	O1	11655011	Mn1	3556051	125.365
Mo1	O1	11555051	O1	11555011	180.000
Bi1	O1	9565041	O1	9555011	80.618
Mo1	O1	9655021	O1	9665031	188.034

### Conclusion

Laboratory X-ray diffractometer provide data that are good enough to obtain structural parameters, as shown in the example of  $\text{Bi}_{0.5}\text{Mn}_{0.64}\text{Mo}_{1.5}\text{O}_{0.41}$ . The possibility to solve ab initio structures from powder diffraction data should not distract from a great number of problems. The quality of the crystalline powder, mainly the coherence length, is crucial to obtain suitable patterns. Powders with coherence length of ca. 100 nm for the crystals are in the lower range of possible candidates for ab initio XRD structure analysis. If the crystals are too small, chemists must make an effort at trying crystal growth techniques using mineralizers or stabilizers at the risk of introducing impurities. A bottleneck is the indexing stage that often requires a trial and error approach. Too many or too few reflections lead to no results. Unambiguously determining unit cell and likely space groups requires experience supported by high resolution diffraction patterns and (new) robust indexing strategies. The number of degrees of freedom in the refinement may then give a limit to the complexity of systems. The type of optimization algorithm in real and reciprocal space – nowadays available – needs a reduction in the range of parameter space. Rigid bodies in real space help solve the structure and during a refinement without constraints indicate the robustness of a model. In summary, the well-balanced quaternary transition metal structure type of  $\text{Bi}_{0.5}\text{Mn}_{0.64}\text{Mo}_{1.5}\text{O}_{0.41}$  cathode materials was successfully synthesized using a coprecipitation method. By performing various analysis techniques, we evaluated and confirmed the superiority of ternary metal oxide frameworks. EDX mapping images reveal that the ternary metals of  $\text{Bi}_{0.5}\text{Mn}_{0.64}\text{Mo}_{1.5}\text{O}_{0.41}$  were well distributed throughout the whole particle.

### References

1. Parveen Rathi, Dharam Pal Singh, Parveen Surain, Synthesis, characterization, powder XRD and antimicrobial-antioxidant activity evaluation of trivalent transition metal macrocyclic complexes, *C. R. Chimie* 18 (2015) 430–437
2. Kai Li and Rik Van Deun, Novel Intense Emission-Tunable  $\text{Li}_{1.5}\text{La}_{1.5}\text{WO}_6:\text{Mn}^{4+}, \text{Nd}^{3+}, \text{Yb}^{3+}$  Material with Good Luminescence Thermal Stability for Potential Applications in c-Si Solar Cells and Plant-Cultivation Far-Red-NIR LEDs, *ACS Sustainable Chem. Eng.* 2019, 7, 16284–16294
3. Peng, Q.; Cao, R.; Ye, Y.; Guo, S.; Hu, Z.; Chen, T.; Zheng, G. Photoluminescence properties of broadband deep-red-emitting  $\text{Na}_2\text{MgAl}_{10}\text{O}_{17}:\text{Mn}^{4+}$  phosphor. *J. Alloys Compd.* 2017, 725, 139–144.
4. Liu, Y.; Gao, G.; Huang, L.; Zhu, Y.; Zhang, X.; Yu, J.; Richards, B. S.; Xuan, T.; Wang, Z.; Wang, J. Co-precipitation synthesis and photoluminescence properties of  $\text{BaTiF}_6:\text{Mn}^{4+}$ : an efficient red phosphor for warm white LEDs. *J. Mater. Chem. C* 2018, 6, 127–133.

5. Yu, Y.; Huang, Y.; Zhang, L.; Lin, Z.; Wang, G. Assessment of structure and spectral characteristics of new laser crystal  $\text{Nd}^{3+}:\text{KBaY}(\text{MoO}_4)_3$ . *J. Alloys Compd.* 2015, 651, 164–169.
6. Marciniak, L.; Bednarkiewicz, A.; Hreniak, D.; Streck, W. The influence of  $\text{Nd}^{3+}$  concentration and alkali ions on the sensitivity of non-contact temperature measurements in  $\text{ALaP}_4\text{O}_{12}:\text{Nd}^{3+}$  (A = Li, K, Na, Rb) nanocrystalline luminescent thermometers. *J. Mater. Chem. C* 2016, 4, 11284–11290.
7. Yang, Z.; Yang, J.; Qiu, J.; Song, Z. Comprehensive investigations of near infrared downshift and upconversion luminescence mechanisms in  $\text{Yb}^{3+}$  single-doped and  $\text{Er}^{3+}, \text{Yb}^{3+}$  codoped  $\text{SiO}_2$  inverse opals. *Phys. Chem. Chem. Phys.* 2017, 19, 31997–32006.
8. Ye, S.; Zhou, J.; Wang, S.; Hu, R.; Wang, D.; Qiu, J. Broadband downshifting luminescence in  $\text{Cr}^{3+}-\text{Yb}^{3+}$  codoped garnet for efficient photovoltaic generation. *Opt. Express* 2013, 21, 4167.
9. Reisfeld, R.; Lieblich-Soffer, N. Energy transfer from  $\text{UO}_2^{2+}$  to  $\text{Sm}^{3+}$  in phosphate glass. *J. Solid State Chem.* 1979, 28, 391–395.
10. Dexter, D. L.; Schulman, J. H. Theory of Concentration Quenching in Inorganic Phosphors. *J. Chem. Phys.* 1954, 22, 1063–1070.
- (49) Blasse, G.; Grabmaier, B. C. *Luminescent Materials*; Springer-Verlag: Berlin, Germany, 1994.
11. Wu, L.; Bai, Y.; Wu, L.; Yi, H.; Zhang, X.; Zhang, L.; Kong, Y.; Zhang, Y.; Xu, J. Analysis of the structure and abnormal photoluminescence of a red-emitting  $\text{LiMgBO}_3:\text{Mn}^{2+}$  phosphor. *Dalton Trans.* 2018, 47, 13094–13105.
12. Parashuram Mishra Synthesis, crystal structure determination and ionic properties of novel  $\text{BiCa}_{0.5}\text{Mg}_{0.5}\text{O}_{2.5}$  via X-ray powder diffraction data, *Elixir Crystal Growth*. 2041 32 (2011) 2041-2045.
13. T. Dan Vu, Firas Krichen, Maud Barre,† Sandrine Coste,† Alain Jouanneaux, Emmanuelle Suard, Andrew Fitch, and François Goutenoire Ab Initio Structure Determination of  $\text{La}_{34}\text{Mo}_8\text{O}_{75}$  Using Powder X-ray and Neutron Diffraction Data, DOI: 10.1021/acs.cgd.8b01552 *Cryst. Growth Des.* XXXX, XXX, XXX–XXX
14. Chambrier, M.-H.; Le Bail, A.; Giovannelli, F.; Redjaimia, A.; Florian, P.; Massiot, D.; Suard, E.; Goutenoire, F.  $\text{La}_{10}\text{W}_2\text{O}_{21}$ : An Anion-Deficient Fluorite-Related Superstructure with Oxide Ion Conduction. *Inorg. Chem.* 2014, 53, 147–159.
15. Lopez-Vergara, A.; Porras-Vazquez, J. M.; Infantes-Molina, A.; Canales-Vazquez, J.; Cabeza, A.; Losilla, E. R.; Marero-Lopez, D. Effect of Preparation Conditions on the Polymorphism and Transport Properties of  $\text{La}_{6-x}\text{MoO}_{12-\delta}$  ( $0 \leq x \leq 0.8$ ). *Chem. Mater.* 2017, 29, 6966–6975.
16. Dmitri O. Charkin, Andrey S. Karpov, Sergey M. Kazakov, Igor V. Plokhikh, Anastasiya I. Zadaya, Alexey N. Kuznetsov, Konstantin I. Maslakov, Anton Yu Teterin, Yury A. Teterin, Alexander N. Zaloga, Oleg I. Siidra, c, f Synthesis, crystal structure, spectroscopic properties, and thermal behavior of rare-earth oxide selenates,  $\text{Ln}_2\text{O}_2\text{SeO}_4$  (Ln  $\frac{1}{4}$  La, Pr, Nd): The new perspectives of solid-state double-exchange synthesis, *Journal of Solid State Chemistry* 277 (2019) 163–168